Improved SMAP Dual-Channel Algorithm for the Retrieval of Soil Moisture

Improved SMAP Dual-Channel Algorithm for the Retrieval of Soil Moisture

Mario Julian Chaubell, Simon H. Yueh, *Fellow, IEEE*, R. Scott Dunbar, Andreas Colliander, *Senior Member, IEEE*, Fan Chen, Steven K. Chan, *Senior Member, IEEE*, Dara Entekhabi, *Fellow, IEEE*, Rajat Bindlish, *Senior Member, IEEE*, Peggy E. O'Neill, *Fellow, IEEE*, Jun Asanuma, Aaron A. Berg, David D. Bosch, Todd Caldwell, Michael H. Cosh, *Senior Member, IEEE*, Chandra Holifield Collins, Jose Martínez-Fernández, Mark Seyfried, Patrick J. Starks, Zhongbo Su, Marc Thibeault, and Jeffrey Walker

***Abstract*— The soil moisture active passive (SMAP) mission was designed to acquire L-band radiometer measurements for the estimation of soil moisture (SM) with an average ubRMSD of not more than 0.04 m^3/m^3 volumetric accuracy in the top 5 cm for vegetation with a water content of less than 5 kg/m^2. Single-channel algorithm (SCA) and dual-channel algorithm (DCA) are implemented for the processing of SMAP radiometer data. The SCA using the vertically polarized brightness temperature (SCA-V) has been providing satisfactory SM retrievals. However, the DCA using prelaunch design and algorithm parameters for vertical and horizontal polarization data has a marginal performance. In this article, we show that with the updates of the roughness parameter h and the polarization mixing parameters Q, a modified DCA (MDCA) can achieve improved accuracy over DCA; it also allows for the retrieval of vegetation optical depth (VOD or τ). The retrieval performance of MDCA is assessed and compared with SCA-V and DCA using four years (April 1, 2015 to March 31, 2019) of *in situ* data from core validation sites (CVSs) and sparse networks. The assessment shows that SCA-V still outperforms all the implemented algorithms.**

***Index Terms*— Dual-channel algorithm (DCA), soil moisture active passive (SMAP), soil moisture (SM) retrieval, vegetation optical depth (VOD) retrieval.**

Manuscript received August 8, 2019; revised October 24, 2019; accepted November 9, 2019. This work was carried out by the Jet Propulsion Laboratory, California Institute of Technology, under a contract with the National Aeronautics and Space Administration. The University of Salamanca team managing the validation site REMEDHUS was supported by the Spanish Ministry of Science, Innovation and Universities with the project ESP2017-89463-C3-3-R, and the European Regional Development Fund (ERDF). *(Corresponding author: Mario Julian Chaubell.)*

Mario Julian Chaubell, Simon H. Yueh, R. Scott Dunbar, Andreas Colliander, and Steven K. Chan are with the Jet Propulsion Laboratory, California Institute of Technology, Pasadena, CA 91109 USA (e-mail: julian@jpl.nasa.gov; simon.yueh@jpl.nasa.gov; roy.s.dunbar@jpl.nasa.gov; andreas.colliander@jpl.nasa.gov; steventsz.k.chan@jpl.nasa.gov).

Fan Chen is with SSAL Inc., Greenbelt, MD 20770 USA, and also with the USDA Agricultural Research Service, Beltsville, MD 20705 USA (e-mail: fan.chen@ars.usda.gov).

Dara Entekhabi is with the Massachusetts Institute of Technology, Cambridge, MA 02139 USA (e-mail: darae@mit.edu).

Rajat Bindlish and Peggy E. O'Neill are with the Goddard Space Flight Center, Greenbelt, MD 20771 USA (e-mail: rajat.bindlish@nasa.gov; peggy.e.oneill@nasa.gov).

Jun Asanuma is with the Center for Research in Isotopes and Environmental Dynamics (CRiED), Tsukuba University, Tsukuba 305-8577, Japan (e-mail: asanuma@ied.tsukuba.ac.jp).

Aaron A. Berg is with the University of Guelph, Guelph, ON N1G 2W1, Canada (e-mail: aberg@uoguelph.ca).

David D. Bosch is with the USDA-ARS Southeast Watershed Research Laboratory, Tifton, GA 31794 USA (e-mail: david.bosch@ars.usda.gov).

Todd Caldwell is with the U.S. Geological Survey, Nevada Water Science Center, Carson City, NV 89701 USA (e-mail: tcaldwell@usgs.gov).

Michael H. Cosh is with the USDA-ARS Hydrology and Remote Sensing Laboratory, Beltsville, MD 20705 USA (e-mail: michael.cosh@usda.gov).

Chandra Holifield Collins is with the USDA-ARS Southwest Watershed Research Center, Tucson, AZ 85719 USA (e-mail: chandra.holifield@ars.usda.gov).

Jose Martínez-Fernández is with the Instituto Hispano Luso de Investigaciones Agrarias (CIALE), Universidad de Salamanca, 37185 Salamanca, Spain (e-mail: jmf@usal.es).

Mark Seyfried is with the USDA-ARS Northwest Watershed Research Center, Boise, ID 83712 USA (e-mail: mark.seyfried@ars.usda.gov).

Patrick J. Starks is with the Grazinglands Research Laboratory, El Reno, OK 73036 USA (e-mail: patrick.starks@usda.gov).

Zhongbo Su is with the ITC Faculty, University of Twente, 7522 NB Enschede, The Netherlands (e-mail: z.su@utwente.nl).

Marc Thibeault is with the SAOCOM Project Science Group, Comisión Nacional de Actividades Espaciales (CONAE), CABA C1063ACH, Argentina (e-mail: mthibeault@conae.gov.ar).

Jeffrey Walker is with Monash University, Melbourne, VIC 3800, Australia (e-mail: jeff.walker@monash.edu.au).

Color versions of one or more of the figures in this article are available online at http://ieeexplore.ieee.org.

Digital Object Identifier 10.1109/TGRS.2019.2959239

I. Introduction

THE soil moisture active passive (SMAP) mission was designed to improve scientific understanding of the global linkages between the land branches of the water, energy, and carbon cycles. Its science products also have applications in mitigating hydrometeorological hazards and enhance climate/weather forecasting. With the goal of obtaining high-accuracy soil moisture (SM) information, the SMAP mission was designed to acquire L-band radiometer measurements for the estimation of SM with an average bias-removed root mean square error (ubRMSE or error standard deviation) of not more than 0.04 m^3/m^3 volumetric accuracy in the top 5 cm for vegetation with water content of less than 5 kg/m^2 [1], [2].

The SMAP mission collects vertically and horizontally polarized brightness temperature data at the incident angle of 40°. The SMAP team implemented several algorithms for the retrieval of SM [2], primarily a single-channel algorithm (SCA) that uses one of the observations to retrieve SM and a dual-channel algorithm (DCA), which uses both polarized brightness observations to retrieve not only SM but also the vegetation optical depth (VOD or τ), a measure of vegetation water content and aboveground vegetation structure. Although dual-polarization was expected to provide additional informa-

tion, the performance of the DCA algorithm has been marginal with higher SM retrieval errors than the SCA-V algorithm [3].

The baseline SMAP retrieval algorithms use the zero-order approximation of the radiative transfer equations, known as the τ-ω emission model [4]. To simulate L-band emission of soil-vegetation systems, the SMAP data processing system assumes a prior value of the effective scattering albedo and roughness parameters based on land cover type and also an estimate of τ based on the normalized difference vegetation index (NDVI) climatology [2]. In this article, we will focus on the selection of the roughness parameters and the albedo, which have been studied by several authors [5]–[7].

The retrieval of τ is of great value for the SMAP mission not only because it will reduce the source of errors on the retrieval of SM (reduces reliance on ancillary data) but it also has significant importance to the science community since it will provide valuable information about the integrated above-ground vegetation moisture state. The estimation of surface SM and τ at a global scale is the main goal for the L-band microwave mission of SMOS (SM and Ocean Salinity) [8]. Recently, Fernandez-Moran *et al.* [9] presented an alternative SMOS product that was developed by Institut National de la Recherche Agronomique (INRA) and Centre d'Etudes Spatiales de la BIOsphère (CESBIO). SMOS-INRA-CESBIO (SMOS-IC) product also provides daily SM and τ at the global scale.

Recent efforts to retrieve SM and τ from SMAP data have been done [10]. Konings *et al.* [10] used a multitemporal DCA (MT-DCA), which assumes that τ changes more slowly than SM and presumably stays almost constant between every two consecutive overpasses. The MT-DCA τ fields and their seasonal dynamics closely follow those estimated using the SMOS multiangular measurements [9]. In addition, the MT-DCA approach allows for the retrieval of a single temporally constant value of the scattering albedo per pixel.

In this article, we show that with the use of suitable roughness parameters and both polarized brightness temperatures (H and V polarization), a modified DCA (MDCA) provides retrieved SM with improvement in accuracy relative to the current DCA. The retrieval performance of MDCA is assessed and compared with SCA-V and DCA using four years (April 1, 2015–March 31, 2019) of *in situ* data from core validation sites (CVSs) [11] and sparse networks representing different seasons and land cover types worldwide.

This article is organized as follows. A background overview of the emission model and algorithms used by SMAP as well as the updates in polarization mixing is provided in Section II. The updates to surface roughness and albedo parameters are described in Section III. The assessment of the retrieval performance is presented in Section IV. A summary is given in Section V.

II. SMAP Algorithms

A. Emission Model

The emission model implemented by SMAP for the retrieval of SM is the well-established τ-ω emission model derived from the radiative transfer equation [2], [4]. The brightness temperature equation, which includes emission components from the soil and the overlying vegetation canopy, is given by

$$\begin{aligned} \mathrm{TB}_p^{\mathrm{sim}} &= T_s e_p \exp(-\tau_p \sec\theta) + T_c(1-\omega_p) \\ &\quad \times [1-\exp(-\tau_p \sec\theta)][1+r_p \exp(-\tau_p \sec\theta)] \end{aligned} \quad (1)$$

where the subscript p refers to polarization (V or H), T_{s} is the soil effective temperature, T_{c} is the vegetation temperature, τ_p is the nadir vegetation opacity, ω_p is the vegetation effective scattering albedo, r_p is the rough soil reflectivity, e_{p} is the rough soil emissivity, and θ is the incidence angle.

The surface roughness reflectivity is modeled by

$$r_p(\theta) = \left[(1-Q)r_p^*(\theta) + Q r_q^*(\theta)\right] e^{(-h\cos^N(\theta))} \quad (2)$$

where Q (polarization decoupling factor), h, and N are the roughness parameters, and $r_p^*(\theta)$ is the Fresnel reflectivity of the smooth surface where the indexes p and q (q opposite to p) account for the polarization V or H. The baseline SMAP implementation of the retrieval algorithms assumes that in (1) $T_{\mathrm{s}} = T_{\mathrm{c}}$ at the early morning descending overpass and that $\omega_{\mathrm{p}} = \omega$ and $\tau_{\mathrm{p}} = \tau$ are polarization independent to reduce the number of algorithm parameters [2].

B. SCA

The SMAP baseline algorithm SCA-V that uses the V-polarized observed brightness temperature $\mathrm{TB}_V^{\mathrm{obs}}$ to retrieve SM minimizes the cost function

$$F(\mathrm{SM}) = \left[\mathrm{TB}_V^{\mathrm{sim}}(\mathrm{SM}) - \mathrm{TB}_V^{\mathrm{obs}}\right]^2 \quad (3)$$

where $\mathrm{TB}_V^{\mathrm{sim}}$ is the simulated V-polarized brightness temperature from the τ-ω emission model. To simulate the L-band emission of the soil-vegetation using (1) and (2), several parameters need to be assumed: a prior value of an estimate of τ based on the NDVI vegetation water content (VWC) climatology, the scattering albedo and the roughness parameter all based on land cover type following the classification scheme of the International Geosphere-Biosphere Programme (IGBP). In addition, the clay fraction, needed to determine the soil dielectric constant, was provided by Harmonized World Soil Database (HWSD), and the land surface temperature, needed to determine the soil effective temperature, was provided by the Global Modeling Assimilation Office (GMAO). Details on the determination of the soil effective temperature can be found in [2]. Recently, a methodology to compute the soil effective temperature was developed in [12], but its applicability was not studied by the SMAP team at this time. For the computation of the dielectric constant, we follow the Mironov model [13], which applies to a wide range of soil types.

The current SMAP SCA-V assumes $N = 2$, the polarization decoupling factor $Q = 0$ and h fields that are fixed for each IGBP classification [2]. At L-band and small values of h, h is related to the root-mean-square of the surface height s as $h = 0.01\ s$ (s in millimeters).

C. DCA

The DCA simultaneously retrieves the SM and τ by minimizing the cost function

$$F_\tau(\mathrm{SM},\tau) = \left[\mathrm{TB}_V^{\mathrm{sim}}(\mathrm{SM},\tau) - \mathrm{TB}_V^{\mathrm{obs}}\right]^2 + \left[\mathrm{TB}_H^{\mathrm{sim}}(\mathrm{SM},\tau) - \mathrm{TB}_H^{\mathrm{obs}}\right]^2 \quad (4)$$

where $\mathrm{TB}_H^{\mathrm{sim}}$ is the simulated H-polarized brightness temperature. Since the launch in 2015, the DCA has been outperformed by the SCA-V.

To improve the DCA, we concentrate on the selection of the roughness parameters, which was the focus of several studies [5], [6], and the update of the parameter ω which represents the effective scattering albedo [14], [15].

The current DCA assumes the same roughness parameters as in the SCA-V, $N = 2$, the polarization decoupling factor $Q = 0$, and h dependent on IGBP classification [2]. In [5] and [6], an alternative model for the selection of the roughness parameter is proposed. Wigneron *et al.* [5] developed an empirical power function between h and s (the root-mean-square of the surface height) based on the PORTOS-1993 experimental data, given by

$$h = \left(\frac{0.9437s}{0.8865s + 2.2913}\right)^6. \quad (5)$$

Furthermore, Lawrence *et al.* [6], based on simulated data from numerical solutions of Maxwell's equations for electromagnetics rough surface scattering model, found that the polarization decoupling factor Q could be related to the h parameter using the linear equation

$$Q = 0.1771h. \quad (6)$$

We will refer to this algorithm as the DCA with Wigneron–Lawrence roughness implementation. The new parametrization of the roughness effect has been evaluated by several authors and is widely used in the literature [7], [15]–[17].

In this article, the Wigneron–Lawrence roughness implementation with $N = 2$ is first tested, and its statistical performance is compared against the baseline SCA-V and the current DCA. This implementation is not the final MDCA introduced in Section III. To make a preliminary evaluation of the impact of using (5) and (6) to retrieve SM, the retrieved SM is compared with the *in situ* measurements at 15 SMAP CVS. For each site, the RMSD, bias, and ubRMSD are computed and then the total average is computed for comparison.

Table I shows the results over all the CVS. We see that the use of the Wigneron–Lawrence roughness model, (5) and (6), outperforms DCA but falls short of meeting the requirement with an ubRMSD = 0.042 $\mathrm{m}^3/\mathrm{m}^3$ (an improvement of ∼14% with respect to DCA ubRMSD) and that SCA-V still shows the best performance over all the statistical parameters. The comparison of SM retrievals versus *in situ* data from the 15 CVS is shown in Fig. 1. The figure on the left shows the current DCA performance and the figure on the right shows the results after the Wigneron–Lawrence roughness implementation. It can be observed that after using the Wigneron–Lawrence roughness implementation, the slope of the scattered data is corrected resulting in a reduction of the bias as seen in Table I.

TABLE I
ALGORITHM ASSESSMENT

Algorithm/stats	ubRMSD ($\mathrm{m}^3/\mathrm{m}^3$)	Bias ($\mathrm{m}^3/\mathrm{m}^3$)	R ($\mathrm{m}^3/\mathrm{m}^3$)
SCA-V	0.038	-0.002	0.816
DCA	0.049	0.038	0.730
Wigneron-Lawrence	0.042	0.004	0.725

Statistics performance comparison for the SMAP baseline algorithms, dca and the Wigneron-Lawrence algorithm based on the SMAP core cal/val sites data. Assessment period from 04/01/2015 to 05/31/2018

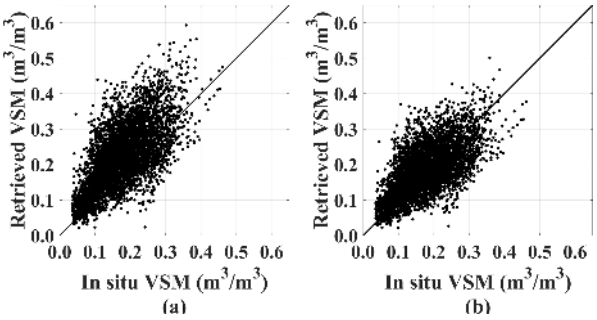

Fig. 1. Scatter plots of SM retrieval versus *in situ* SM data. (Left) Current SMAP DCA algorithm. (Right) Wigneron–Lawrence implementation.

III. ALGORITHM PARAMETERS UPDATE

A. Roughness Surface Parameter h

The limitation of Wigneron–Lawrence parameterization is that it requires prior knowledge of s. To overcome this limitation, we obtain a global map of the roughness parameter h from SMAP data and NDVI VWC climatology as ancillary. The algorithm is explained in the following. Using the cost function

$$F_h(\mathrm{SM},h') = \left[\mathrm{TB}_V^{\mathrm{sim}}(\mathrm{SM},h') - \mathrm{TB}_V^{\mathrm{obs}}\right]^2 + \left[\mathrm{TB}_H^{\mathrm{sim}}(\mathrm{SM},h') - \mathrm{TB}_H^{\mathrm{obs}}\right]^2 \quad (7)$$

as in (6), we retrieved SM and roughness coefficient h' using one year of SMAP data (2017) allowing the generation of a time series of h' for each grid cell *(i, j)* over the 9-km Equal-Area Scalable Earth Grid 2.0 (EASE2) grid. We identify h'(i, j, k) by the time series of h' at the *(i, j)* grid cell and time index k and by τ *(i, j, k)* the associated VOD from NDVI. Defining $\tau_{\min}(i,j) = \min\{\tau(i,j,k), \text{for all } k\}$ and $\tau_{\max}(i,j) = \max\{\tau(i,j,k), \text{for all } k\}$, we compute the values of h over the EASE2 grid as $h(i,j) = \text{average}\ \{h'(i,j,k) : \tau(i,j,k) <= \tau_{\min}(i,j) + f*(\tau_{\max}(i,j) - \tau_{\min}(i,j))\}$ where the factor $f = 0.05$ was selected to assure: 1) that the selection of h' was based on minimum vegetation impact locally and 2) that the set of h' does not contains only the element corresponding to $\tau_{\min}$. The resulting global map of h which we now use as input in our modified-dual channel retrieval algorithm is shown in Fig. 2. It is worth noting that the retrieved global map of h captures the expected topographical features. For example, we can see the Andes in South America, the Rocky Mountains in North America, the Himalayan Mountains in Asia, and some other minor land features along the Red Sea coast and in the Sahara desert such as the Tibesti Mountains.

TABLE II
ALBEDO VALUES

ID	MODIS IGBP land classification	SMAP L2 Baseline	SMAP L4	MTDCA	SMOS-IC	MDCA
0	Water Bodies	0				-
1	Evergreen Needleleaf Forests	0.050	0.11	0.07	0.06	0.07
2	Evergreen Broadleaf Forests	0.050	0.07	0.08	0.06	0.07
3	Deciduous Needleleaf Forests	0.050	0.11	0.06	0.06	0.07
4	Deciduous Broadleaf Forests	0.050	0.09	0.07	0.06	0.07
5	Mixed Forests	0.050	0.10	0.07	0.06	0.07
6	Closed Shrublands	0.050	0.09	0.08	0.10	0.08
7	Open Shrublands	0.050	0.09	0.06	0.08	0.07
8	Woody Savannas	0.050	0.12	0.08	0.06	0.08
9	Savannas	0.080	0.13	0.07	0.10	0.10
10	Grasslands	0.050	0.06	0.06	0.10	0.07
11	Permanent Wetlands	0	0.13	0.16	0.10	0.10
12	Croplands - Average	0.050	0.10	0.10	0.12	0.06
13	Urban and Built-up Lands	0.030	0.10	0.08	0.10	0.08
14	Crop-land/Natural Vegetation Mosaics	0.065	0.14	0.09	0.12	0.10
15	Snow and Ice	0	0.09	0.11	0.10	0.08
16	Barren	0	0.07	0.02	0.12	0.05

Values of albedo obtained from various independent teams and MDCA adopted values.

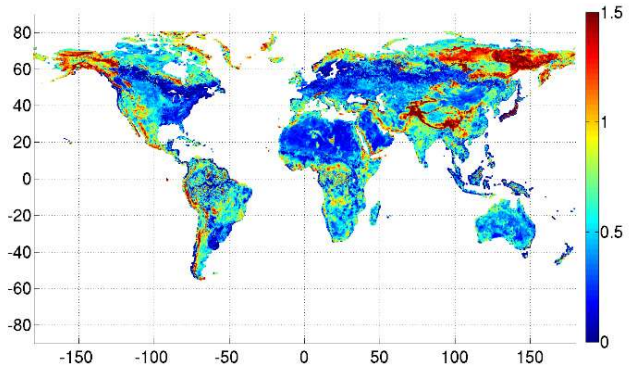

Fig. 2. Global map of the roughness parameter h ancillary file used on the implementation of the MDCA.

B. Effective Scattering Albedo ω

With the generation of h, the implemented model depends only on the estimation of the effective scattering albedo ω which is dependent on the structure and composition of the vegetation and landscape heterogeneity. There have been several studies to quantify the correct values but the results presented in the literature are not consistent [14], [15], and [18].

The current values of albedo (ω) that SMAP uses are provided in Table II (SMAP L2 Baseline), and they are assigned following the IGBP scheme. Based on several independent sources and the accumulation of evidence, we determined that the current values of albedo are likely to be low and they need to be reconsidered. Table II contains the values of albedo proposed by different independent teams (SMAP Level 2 (L2), SMAP Level 4 (L4), SMOS-IC [9], [14], and the multitemporal DCA (MTDCA) [10]). The last column on the right shows the values adopted by SMAP for the MDCA implementation based on the data sources in Table II and major IGBP classes.

IV. RESULTS AND ASSESSMENT

MDCA simultaneously retrieves SM and τ by minimizing the cost function (4) and using (1), (2), and (6) to simulate TB_H^{sim} and TB_V^{sim} together with the parameter h from the ancillary data shown in Fig. 2 and the albedo ω listed in the final column of Table II. Four years (04/01/2015 to 03/31/2019) of averaged SM global maps are shown in Fig. 3. SM retrieved using SCA-V, MDCA, and the differences SCA-V(SM) minus MDCA(SM) are shown from top to bottom, respectively. There is agreement (small wet bias of MDCA with respect to SCA-V) in barren areas and open shrublands. Grasslands show wetter MDCA SM retrievals. SCA-V retrieves higher values of SM in forested areas, woody savannas, and savannas (these last two below 50° latitude). Woody savannas and savannas above 50° latitude show that SCA-V retrieves lower values of SM. Four years of averaged τ global maps are shown in Fig. 4. τ retrieved using SCA-V, MDCA, and the differences NDVI(τ) minus MDCA(τ) are shown from top to bottom, respectively. Forested areas, woody savannas, savannas, and croplands predominately have higher values of NDVI τ except for the east coast of U.S., while barren and grasslands areas show a good agreement between NDVI τ and MDCA retrieved τ.

The SMAP project validates the accuracy of SM products using several sources of information. Among them are CVSs,

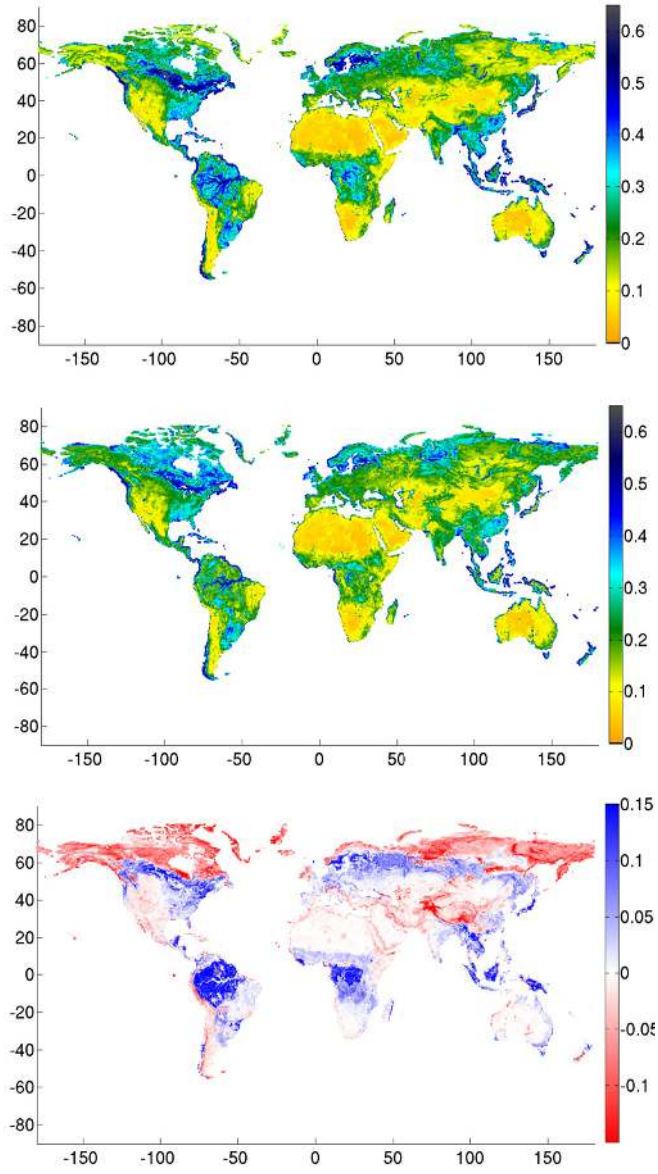

Fig. 3. Global maps of SM temporal mean and differences. (Top) SCA-V. We covered the period from 01/04/2015 to 31/03/2019. (Center) MDCA. (Bottom) SCA-V-MDCA differences.

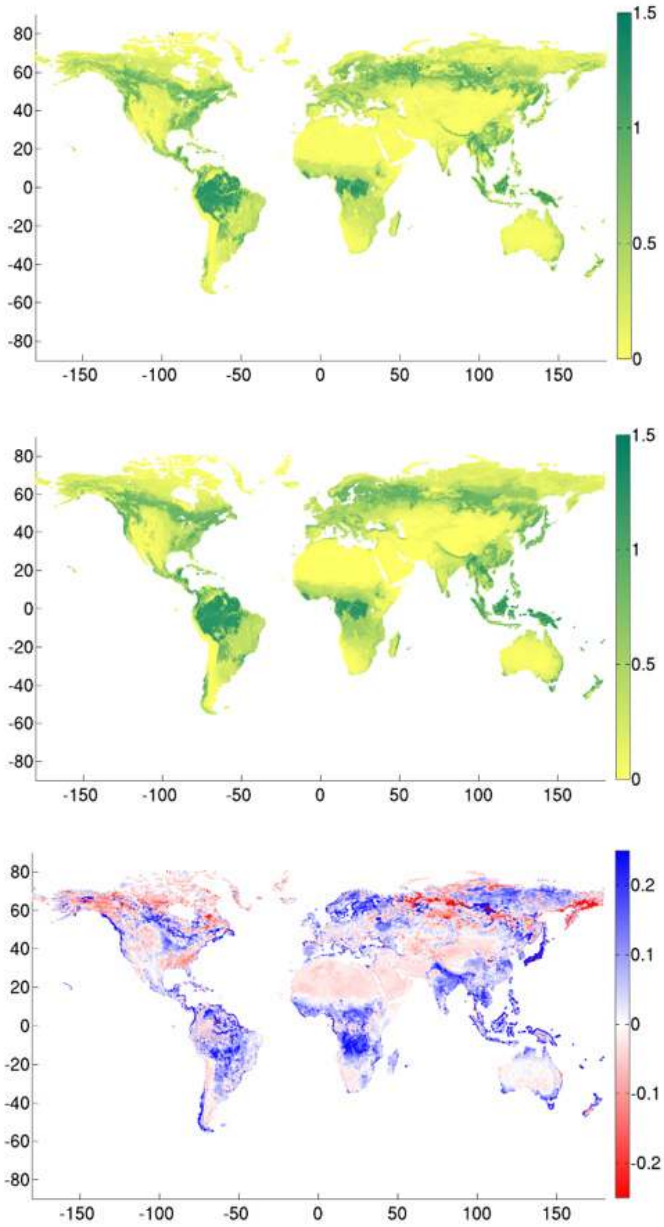

Fig. 4. Global maps of temporal τ mean and differences. (Top) NDVI τ. We covered the period from 01/04/2015 to 31/03/2019. (Center) MDCA τ. (Bottom) NDVI-MDCA τ differences.

which provide the ground-based data in a timely manner to the SMAP project [3], [11], and sparse networks such as the United States Department of Agriculture (USDA) Soil Climate Analysis Network (SCAN) and the National Oceanic and Atmospheric Administration (NOAA) Climate Research Network.

In order to assess the results, four statistical parameters were compared, the ubRMSD, bias, RMSD, and correlation (R). The comparison between DCA (from previous v2 enhanced product release), SCA-V, and MDCA for 15 CVS is presented in Tables III and IV. The assessment for descending passes is presented in Table III, while the assessment for ascending passes is presented in Table IV. The total average for each statistical parameter is shown in the bottom row where we can see that MDCA not only outperforms DCA for all the parameters but also meets the SMAP mission requirements for both descending and ascending passes. Indeed, for descending passes the ubRMSD decreased from 0.049 to 0.040 m^3/m^3(∼18%), the bias decreased from 0.039 to −0.007 m^3/m^3, the RMSD decreased from 0.066 to 0.050 m^3/m^3, and the correlation increased from 0.728 to 0.772. Comparable behaviors are observed for ascending passes. SCA-V outperforms the MDCA algorithm in all cases. The combined scatter plots associated with these results are shown in Fig. 5, which shows retrieved SM versus *in situ* SM at CVS. From left to right, the figure shows the retrieved SM from SCA-V, DCA, and MDCA. We see that from DCA to MDCA there is a correction in slope, and therefore, a correction in bias as can be seen in Tables III and IV. It can also be observed that MDCA corrects the deviation observed in the SCA-V for high *in situ* SM, Fig. 5 (left).

TABLE III
CVS ASSESSMENT

CVS	ubRMSD (m^3/m^3)			Bias (m^3/m^3)			RMSD (m^3/m^3)			R		
	DCA	SCA-V	MDCA	DCA	SCA-V	MDCA	DCA	SCA-V	MDCA	DCA	SCA-V	MDCA
Reynolds Creek	0.055	0.040	0.045	0.036	-0.013	-0.002	0.065	0.042	0.046	0.592	0.653	0.610
Walnut Gulch	0.042	0.026	0.029	0.052	0.015	0.022	0.067	0.030	0.036	0.815	0.796	0.792
TxSON	0.041	0.021	0.030	0.087	-0.008	0.016	0.096	0.023	0.034	0.821	0.934	0.867
Fort Cobb	0.044	0.029	0.034	0.009	-0.047	-0.040	0.045	0.055	0.052	0.813	0.878	0.836
Little Washita	0.042	0.021	0.032	0.055	-0.018	-0.001	0.069	0.028	0.032	0.815	0.912	0.843
South Fork	0.055	0.052	0.053	-0.012	-0.038	-0.057	0.057	0.064	0.078	0.628	0.705	0.636
Little River	0.050	0.036	0.036	0.144	0.059	0.051	0.152	0.069	0.063	0.550	0.783	0.759
Kenaston	0.041	0.031	0.035	0.057	0.007	0.020	0.070	0.031	0.040	0.585	0.774	0.678
Carman	0.066	0.067	0.061	-0.022	-0.050	-0.061	0.070	0.083	0.086	0.488	0.587	0.553
Monte Buey	0.043	0.051	0.038	-0.001	-0.015	-0.039	0.043	0.053	0.054	0.777	0.860	0.789
REMEDHUS	0.053	0.042	0.041	0.038	0.017	0.016	0.065	0.045	0.044	0.818	0.845	0.825
Twente	0.059	0.054	0.049	0.078	0.045	-0.001	0.098	0.071	0.049	0.751	0.889	0.851
HOBE	0.065	0.036	0.051	0.000	-0.003	-0.046	0.065	0.036	0.069	0.755	0.860	0.772
MAHASRI	0.035	0.030	0.030	0.008	0.006	0.009	0.035	0.031	0.032	0.802	0.854	0.845
Yanco	0.046	0.039	0.038	0.064	0.014	0.008	0.079	0.041	0.039	0.915	0.932	0.921
Mean Absolute Bias				0.044	0.024	0.026						
Average	0.049	0.038	0.040	0.039	-0.002	-0.007	0.072	0.047	0.050	0.728	0.817	0.772

CVS assessment for descending passes. The assessment period from 04/01/2015 to 03/31/2019

TABLE IV
CVS ASSESSMENT

CVS	ubRMSD((m^3/m^3)			Bias (m^3/m^3)			RMSD (m^3/m^3)			R		
	DCA	SCA-V	MDCA	DCA	SCA-V	MDCA	DCA	SCA-V	MDCA	DCA	SCA-V	MDCA
Reynolds Creek	0.053	0.043	0.045	0.044	-0.015	-0.001	0.069	0.045	0.045	0.621	0.623	0.623
Walnut Gulch	0.038	0.024	0.028	0.034	0.003	0.009	0.051	0.024	0.029	0.730	0.751	0.745
TxSON	0.035	0.020	0.028	0.081	-0.006	0.010	0.089	0.021	0.030	0.822	0.935	0.860
Fort Cobb	0.038	0.030	0.030	-0.007	-0.049	-0.049	0.038	0.057	0.058	0.795	0.873	0.837
Little Washita	0.037	0.022	0.029	0.045	-0.012	-0.006	0.058	0.025	0.030	0.788	0.912	0.817
South Fork	0.058	0.046	0.056	-0.027	-0.044	-0.063	0.064	0.063	0.085	0.608	0.770	0.645
Little River	0.059	0.036	0.041	0.134	0.061	0.048	0.146	0.071	0.063	0.314	0.764	0.635
Kenaston	0.047	0.025	0.040	0.056	0.007	0.016	0.073	0.026	0.043	0.665	0.884	0.727
Carman	0.055	0.052	0.050	-0.031	-0.053	-0.068	0.064	0.074	0.084	0.550	0.656	0.594
Monte Buey	0.040	0.043	0.037	-0.015	-0.006	-0.048	0.043	0.043	0.061	0.773	0.917	0.775
REMEDHUS	0.050	0.041	0.041	0.027	0.007	0.007	0.057	0.041	0.041	0.817	0.834	0.810
Twente	0.050	0.052	0.043	0.062	0.050	-0.008	0.080	0.072	0.044	0.814	0.910	0.876
HOBE	0.063	0.034	0.050	0.006	0.006	-0.041	0.064	0.035	0.065	0.767	0.849	0.783
MAHASRI	0.035	0.031	0.032	0.000	0.000	0.000	0.035	0.031	0.032	0.681	0.757	0.747
Yanco	0.040	0.041	0.037	0.053	0.016	0.004	0.066	0.044	0.037	0.936	0.936	0.924
Mean Absolute Bias				0.041	0.022	0.025						
Average	0.047	0.036	0.039	0.031	-0.002	-0.013	0.066	0.045	0.050	0.712	0.825	0.760

CVS assessment for ascending passes. The assessment period from 04/01/2015 to 03/31/2019

TABLE V
STATISTICAL COMPARISON BETWEEN SCA-V SM AND MDCA SM

CVS	Mean diff (m^3/m^3)	Mean diff error (m^3/m^3)	ubRMSD (m^3/m^3)	ubRMSD error (m^3/m^3)	Corr	Corr LB	Corr UB	t	N
Reynolds Creek	0.016	±0.003	0.014	±0.000	0.986	0.985	0.988	7.467*	1259
Walnut Gulch	0.007	±0.003	0.007	±0.000	0.996	0.995	0.996	3.669*	1212
TxSON	0.020	±0.004	0.021	±0.001	0.938	0.931	0.944	9.203*	1227
Fort Cobb	0.004	±0.004	0.021	±0.001	0.947	0.941	0.952	1.740	1357
Little Washita	0.013	±0.004	0.026	±0.001	0.907	0.897	0.916	5.956*	1374
South Fork	0.007	±0.005	0.030	±0.001	0.910	0.898	0.921	2.186*	875
Little River	-0.010	±0.004	0.024	±0.001	0.929	0.922	0.937	3.855*	1311
Kenaston	0.016	±0.005	0.030	±0.001	0.887	0.874	0.900	5.944*	1063
Carman	0.010	±0.007	0.033	±0.001	0.920	0.909	0.930	2.567*	796
Monte Buey	0.001	±0.005	0.034	±0.001	0.884	0.869	0.898	0.392	891
REMEDHUS	0.001	±0.004	0.011	±0.000	0.988	0.987	0.990	0.268	1504
Twente	-0.046	±0.006	0.025	±0.001	0.971	0.968	0.974	13.032*	1594
HOBE	-0.004	±0.004	0.029	±0.001	0.920	0.912	0.927	1.526	1687
MAHASRI	0.001	±0.003	0.005	±0.000	0.995	0.995	0.996	0.534	1009
Yanco	-0.006	±0.006	0.025	±0.001	0.980	0.977	0.982	1.489	1358

Statistical comparison between SCA-V SM and MDCA SM. Statistical confidence limits at the 95% level. Statistics with significant differences are marked by * symbol

TABLE VI
SPARSE NETWORK ASSESSMENT

SMAP Enhanced Product V3													
Descending (AM)	RMSD (m^3/m^3)			ubRMSD (m^3/m^3)			Bias (m^3/m^3)			R			
	DCA	SCA-V	MDCA	DCA	SCA-V	MDCA	DCA	SCA-V	MDCA	DCA	SCA-V	MDCA	N sites
Evergreen needleleaf forest	0.103	0.049	0.067	0.049	0.034	0.036	0.090	0.031	0.057	0.571	0.736	0.693	2
Mixed forest	0.081	0.060	0.063	0.066	0.057	0.060	0.047	-0.019	-0.020	0.579	0.680	0.647	1
Open shrublands	0.079	0.055	0.061	0.049	0.041	0.046	0.049	0.000	0.018	0.540	0.593	0.583	43
Woody savannas	0.140	0.088	0.088	0.072	0.056	0.060	0.108	0.028	0.023	0.497	0.732	0.657	19
Savannas	0.063	0.052	0.052	0.039	0.031	0.031	0.012	-0.006	-0.014	0.859	0.876	0.870	3
Grasslands	0.084	0.072	0.072	0.058	0.050	0.054	0.035	-0.027	-0.011	0.644	0.696	0.666	238
Croplands	0.105	0.098	0.098	0.072	0.066	0.066	0.032	-0.011	-0.011	0.519	0.601	0.555	61
Crop/Natural vegetation mosaic	0.122	0.090	0.091	0.070	0.063	0.065	0.081	0.017	0.007	0.548	0.644	0.636	23
Barren/Sparse	0.067	0.035	0.040	0.029	0.023	0.025	0.058	0.014	0.024	0.539	0.633	0.638	6
Average	0.094	0.066	0.070	0.056	0.047	0.049	0.057	0.003	0.008	0.588	0.688	0.660	396
Ascending (PM)	RMSD (m^3/m^3)			ubRMSD (m^3/m^3)			Bias (m^3/m^3)			R			
	DCA	SCA-V	MDCA	DCA	SCA-V	MDCA	DCA	SCA-V	MDCA	DCA	SCA-V	MDCA	N sites
Evergreen needleleaf forest	0.120	0.055	0.078	0.053	0.036	0.042	0.107	0.034	0.066	0.403	0.655	0.594	2
Mixed forest	0.077	0.056	0.057	0.057	0.055	0.055	0.052	-0.013	-0.017	0.694	0.727	0.728	1
Open shrublands	0.083	0.054	0.061	0.050	0.041	0.046	0.052	-0.003	0.016	0.466	0.560	0.535	43
Woody savannas	0.140	0.091	0.088	0.073	0.055	0.061	0.107	0.037	0.023	0.452	0.712	0.606	19
Savannas	0.067	0.055	0.056	0.041	0.033	0.034	0.016	-0.001	-0.013	0.814	0.850	0.835	3
Grasslands	0.084	0.072	0.073	0.057	0.049	0.053	0.032	-0.025	-0.014	0.634	0.701	0.662	238
Croplands	0.102	0.097	0.097	0.069	0.064	0.064	0.025	-0.006	-0.016	0.513	0.605	0.547	61
Crop/Natural vegetation mosaic	0.117	0.091	0.091	0.069	0.063	0.065	0.075	0.030	0.007	0.531	0.633	0.604	23
Barren/Sparse	0.075	0.036	0.041	0.033	0.025	0.027	0.067	0.014	0.025	0.356	0.514	0.496	6
Average	0.096	0.067	0.071	0.056	0.047	0.049	0.059	0.007	0.009	0.540	0.662	0.623	396

The assessment report over the sparse networks using 48 months of SMAP SM data. The accuracy of three algorithms, MDCA, SCA-V and DCA (from previous SMAP product release) is compared. The top section assesses the descending over passes and the bottom section assesses the ascending over passes.

The results show SCA-V SM and MDCA SM have comparable performance statistics when compared with the 15 CVS. In order to assess the statistical significance of the differences, we perform statistical significance tests on the statistics. We analyze the statistics at a 95% confidence level of the difference between the time series SCA-V SM and time series MDCA SM at the 15 CVS. Table V shows from left to right, the mean difference, the mean difference error, ubRMSD, ubRMSD error, the correlation, the correlation lower bound (LB), the correlation upper bound (UB), the t-value, and the number of samples (N). Table V shows that the mean difference only exceeds 0.04 m^3/m^3at Twente, the ubRMSD stays below the 0.04 m^3/m^3 at all the CVS and the correlation is high, greater than 0.85 in all cases. The t-value was also computed as

$$t = \frac{\bar{x} - \bar{y}}{\sqrt{\frac{\sigma_x}{N} + \frac{\sigma_y}{N}}} \tag{8}$$

where $\bar{x}$ is the mean of MDCA SM, $\bar{y}$ is the mean of SCA-V SM, σ_x and σ_y are the respective variances, and N is the

TABLE VII
MDCA AND NDVI TAU AT NADIR

		MDCA τ			NDVI τ		
ID	MODIS IGBP land classification	mean	std	median	mean	std	median
1	Evergreen Needleleaf Forests	0.51	0.16	0.54	0.55	0.14	0.59
2	Evergreen Broadleaf Forests	0.74	0.21	0.80	0.82	0.16	0.90
3	Deciduous Needleleaf Forests	0.34	0.12	0.37	0.42	0.06	0.44
4	Deciduous Broadleaf Forests	0.53	0.14	0.54	0.58	0.12	0.60
5	Mixed Forests	0.53	0.16	0.55	0.57	0.12	0.60
6	Closed Shrublands	0.14	0.06	0.14	0.16	0.05	0.15
7	Open Shrublands	0.10	0.09	0.06	0.09	0.07	0.07
8	Woody Savannas	0.32	0.11	0.31	0.38	0.09	0.39
9	Savannas	0.23	0.08	0.23	0.27	0.07	0.28
10	Grasslands	0.08	0.07	0.06	0.09	0.08	0.07
11	Permanent Wetlands	0.14	0.14	0.10	0.15	0.12	0.13
12	Croplands - Average	0.15	0.09	0.14	0.21	0.08	0.20
13	Urban and Built-up Lands	0.24	0.15	0.23	0.30	0.13	0.30
14	Crop-land/Natural Vegetation Mosaics	0.31	0.13	0.30	0.34	0.12	0.33
15	Snow and Ice	0.08	0.08	0.05	0.05	0.07	0.02
16	Barren	0.02	0.01	0.02	0.00	0.01	0.00

MDCA and NDVI tau at nadir grouped by land cover types. Statistics over 4 years of data from 01/04/2015 to 31/03/2019. The data was not filtered using the retrieval quality flag.

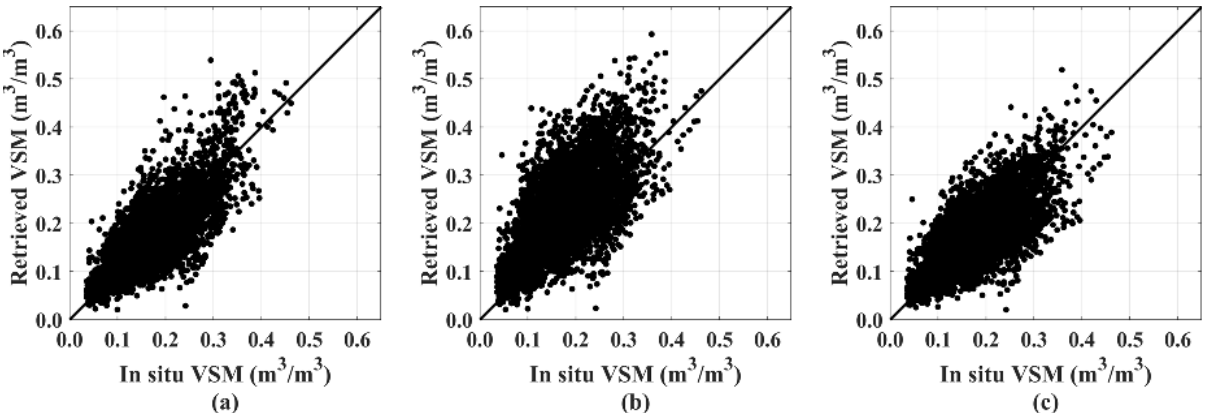

Fig. 5. Scatter SM retrieval versus CVS *in situ* SM. (Left) SCA-V. (Center) DCA. (Right) MDCA.

number of samples. Considering that the critical t value for a two-tailed distribution is $\sim$1.96, Table V shows that for 9 of the 15 CVS, the differences are statistically significant (marked by $*$ in Table V) while for 6 of them the differences are not statistically significant.

The assessment report over the sparse networks using 48 months of SMAP SM data is presented in Table VI. The accuracy of three algorithms, MDCA, SCA-V, and DCA (from previous SMAP product release), is compared. The ubRMSD, bias, RMSD, and correlation (R) for several land types and for descending passes (top part of Table VI) and ascending passes (bottom of Table VI) are presented. We observe that SCA-V outperforms the two DCAs but we can also see that MDCA shows improvement with respect to DCA for all the statistical parameters.

Due to the lack of *in situ* measurements to be used as references, the assessment of the accuracy of the retrieved τ values on a global scale is not simple and thus no quantitative

assessment of the SMAP MDCA τ is given. The retrieved values of τ shown in Fig. 4 (top) are lower than those reported in [9], [10], and [19]. The global median value of the MDCA τ is 0.26, lower than the 0.33 reported in [10]. The global mean and standard deviation (std) are 0.36 and 0.33, respectively. The data were not filtered using the quality flags but all the data with values higher than $\tau = 2$ were considered anomalous and discarded. Mean, std, and median for the retrieved τ and NDVI τ by land cover types are presented in Table VII.

V. Conclusion

In this article, we show that by choosing a suitable set of roughness parameters and adjusted albedo values, and MDCA allows for an accurate retrieval of SM. We show that MDCA retrievals of SM not only outperform DCA but also the retrieved SM meets the SMAP mission requirements for ascending and descending passes. We also show that, even though the retrieved SM using SCA-V performs slightly better when compared with *in situ* and sparse network data, the MDCA is a reliable SM set of data retrieved simultaneously with τ and the additional information may be of interest for several research groups [20]–[22]. All radiometer data products from SMAP can be obtained from the National Snow and Ice Data Center (NSIDC DAAC, http://nsidc.org/data/SMAP/).

Acknowledgment

The authors would like to thank Karsten Jensen of the University of Copenhagen, Denmark, and Heather McNairn and Jarrett Powers of the Agriculture and Agri-Food Canada (AAFC) for their work managing the CVSs, HOBE, and Carman, respectively.

References

[1] D. Entekhabi *et al.*, "Neill, K. Kellogg, "The soil moisture active passive (SMAP) mission," *Proc. IEEE*, vol. 98, no. 5, pp. 704–716, May 2010, doi: 10.1109/JPROC.2010.2043918.

[2] P. O'Neill, E. Njoku, T. Jackson, S. Chan, and R. Bindlish, "SMAP algorithm theoretical basis document: Level 2 & 3 soil moisture (passive) data products," Ph.D. dissertation, Jet Propuls. Lab., California Inst. Technol., Pasadena, CA, USA, 2015.

[3] S. K. Chan *et al.*, "Neill, "Development and assessment of the SMAP enhanced passive soil moisture product," *Remote Sens. Environ.*, vol. 204, pp. 931–941, Jan. 2018, doi: /10.1016/j.rse.2017.08.025.

[4] T. Mo, B. J. Choudhury, T. J. Schmugge, J. R. Wang, and T. J. Jackson, "A model for microwave emission from vegetation-covered fields," *J. Geophys. Res., Oceans*, vol. 87, no. C13, pp. 11229–11237, Dec. 1982.

[5] J. Wigneron *et al.*, "Evaluating an improved parameterization of the soil emission in L-MEB," *IEEE Trans. Geosci. Remote Sens.*, vol. 49, no. 4, pp. 1177–1189, Apr. 2011, doi: 10.1109/TGRS.2010.2075935.

[6] H. Lawrence, J.-P. Wigneron, F. Demontoux, A. Mialon, and Y. H. Kerr, "Evaluating the semiempirical H–Q model used to calculate the L-band emissivity of a rough bare soil," *IEEE Trans. Geosci. Remote Sens.*, vol. 51, no. 7, pp. 4075–4084, Jul. 2013, doi: 10.1109/TGRS.2012.2226995.

[7] D. Zheng *et al.*, "Impact of surface roughness, vegetation opacity and soil permittivity on L-band microwave emission and soil moisture retrieval in the third pole environment," *Remote Sens. Environ.*, vol. 209, pp. 633–647, May 2018, doi: 10.1016/j.rse.2018.03.011.

[8] Y. H. Kerr *et al.*, "The SMOS soil moisture retrieval algorithm," *IEEE Trans. Geosci. Remote Sens.*, vol. 50, no. 5, pp. 1384–1403, May 2012, doi: 10.1109/TGRS.2012.2184548.

[9] R. Fernandez-Moran *et al.*, "SMOS-IC: An alternative SMOS soil moisture and vegetation optical depth product," *Remote Sens.*, vol. 9, no. 5, p. 457, 2017, doi: 10.3390/rs9050457.

[10] A. G. Konings, M. Piles, N. Das, and D. Entekhabi, "L-band vegetation optical depth and effective scattering albedo estimation from SMAP," *Remote Sens. Environ.*, vol. 198, pp. 460–470, Sep. 2017, doi: 10.1016/j.rse.2017.06.037.

[11] A. Colliander *et al.*, "Validation of SMAP surface soil moisture products with core validation sites," *Remote Sens. Environ.*, vol. 191, pp. 215–231, Mar. 2017.

[12] S. Lv, Y. Zeng, Z. Su, and J. Wen, "A closed-form expression of soil temperature sensing depth at L-band," *IEEE Trans. Geosci. Remote Sens.*, vol. 57, no. 7, pp. 4889–4897, Jul. 2019, doi: 10.1109/TGRS.2019.2893687.

[13] V. L. Mironov, L. G. Kosolapova, and S. V. Fomin, "Physically and mineralogically based spectroscopic dielectric model for moist soils," *IEEE Trans. Geosci. Remote Sens.*, vol. 47, no. 7, pp. 2059–2070, Jul. 2009.

[14] R. Fernandez-Moran *et al.*, "Calibrating the effective scattering albedo in the SMOS algorithm: Some first results," in *Proc. IEEE Int. Geosci. Remote Sens. Symp. (IGARSS)*, Beijing, China, vol. 16, Jul. 2016, pp. 826–829.

[15] J.-P. Wigneron *et al.*, "Modelling the passive microwave signature from land surfaces: A review of recent results and application to the L-band SMOS & SMAP soil moisture retrieval algorithms," *Remote Sens. Environ.*, vol. 192, pp. 238–262, Apr. 2017, doi: 10.1016/j.rse.2017.01.024.

[16] R. Fernandez-Moran *et al.*, "Roughness and vegetation parameterizations at L-band for soil moisture retrievals over a vineyard field," *Remote Sens. Environ.*, vol. 170, pp. 269–279, Dec. 2015, doi: 10.1016/j.rse.2015.09.006.

[17] B. Montpetit, A. Royer, J.-P. Wigneron, A. Chanzy, and A. Mialon, "Evaluation of multi-frequency bare soil microwave reflectivity models," *Remote Sens. Environ.*, vol. 162, pp. 186–195, Jun. 2015.

[18] M. Kurum, "Quantifying scattering albedo in microwave emission of vegetated terrain," *Remote Sens. Environ.*, vol. 129, pp. 66–74, Feb. 2013, doi: 10.1016/j.rse.2015.02.015.

[19] J. P. Grant *et al.*, "Comparison of SMOS and AMSR-E vegetation optical depth to four MODIS-based vegetation indices," *Remote Sens. Environ.*, vol. 172, pp. 87–100, Jan. 2016, doi: 10.1016/j.rse.2015.10.021.

[20] A. F. Feldman, "Moisture pulse-reserve in the soil-plant continuum observed across biomes," *Nature Plants*, vol. 4, pp. 1026–1033, Dec. 2018, doi: 10.1038/s41477-018-0304-9.

[21] A. G. Konings, K. Rao, and S. C. Steele-Dunne, "Macro to micro: Microwave remote sensing of plant water content for physiology and ecology," *New Phytologist*, vol. 223, no. 3, pp. 1166–1172, 2019, doi: 10.1111/nph.15808.

[22] K. Rao, W. R. L. Anderegg, A. Sala, J. Martínez-Vilalta, and A. G. Konings, "Satellite-based vegetation optical depth as an indicator of drought-driven tree mortality," *Remote Sens. Environ.*, vol. 227, pp. 125–136, Jun. 2019, doi: 10.1016/j.rse.2019.03.026.

Mario Julian Chaubell received the B.Sc. degree in mathematics from the National University of Mar del Plata, Buenos Aires, Argentina, in 1997, and the Ph.D. degree in applied and computational mathematics from the California Institute of Technology, Pasadena, CA, USA, in 2004. His doctoral work focused on low-coherence interferometric imaging.

In April 2004, he joined the Jet Propulsion Laboratory (JPL), Pasadena, as a Post-Doctoral Research Associate in the tracking systems and applications section, where he worked on the modeling of EM-wave propagation in fully 3-D atmospheric refractive index distributions. In April 2007, he joined the Radar Science and Engineering Section, JPL, as a Permanent Employee, where he has been working on the forward modeling of radar and radiometer measurements and retrieval of the geophysical quantity from those measurements. He has also been involved in electromagnetic modeling of electrically large aperture systems and structures. He was a part of the SMAP Instrument Operations Team and SMAP Radar L1 Subsystem Team. He is currently a part of the SMAP Radiometer L1 Team and SMAP Soil Moisture L2 Team.

Simon H. Yueh (Fellow, IEEE) received the Ph.D. degree in electrical engineering from the Massachusetts Institute of Technology, Cambridge, MA, USA, in January 1991.

He was a Post-Doctoral Research Associate with the Massachusetts Institute of Technology from February to August 1991. In September 1991, he joined the Radar Science and Engineering Section, Jet Propulsion Laboratory (JPL), Pasadena, CA, USA, where he has assumed various engineering and science management responsibilities. He served as a Project Scientist of the National Aeronautics and Space Administration (NASA) Aquarius mission from January 2012 to September 2013, the Deputy Project Scientist of NASA Soil Moisture Active Passive Mission from January 2013 to September 2013, and has been the SMAP Project Scientist since October 2013. He has been the Principal/Co-Investigator of numerous NASA and DOD research projects on remote sensing of ocean salinity, ocean wind, terrestrial snow, and soil moisture. He has authored four book chapters and published more than 200 publications and presentations.

Dr. Yueh is a member of the American Geophysical Union and the URSI Commission F. He received the 2014 IEEE GRSS Transaction Prize Paper Award, the 2010 IEEE GRSS Transaction Prize Paper Award, the 2002 IEEE GRSS Transaction Prize Paper Award, the 2000 Best Paper Award in the IEEE International Geoscience and Remote Symposium 2000, and the 1995 IEEE GRSS Transaction Prize Paper Award for an article on polarimetric radiometry. He also received the JPL Lew Allen Award in 1998, the JPL Ed Stone Award in 2003, the NASA Exceptional Technology Achievement Award in 2014, and the NASA Outstanding Public Leadership Medal in 2017. He was an Associate Editor of *Radio Science* from 2003 to 2007. He is the Editor-in-Chief of the IEEE TRANSACTIONS OF GEOSCIENCE AND REMOTE SENSING.

R. Scott Dunbar received the B.S. degree in physics and astronomy from the University of Albany, Albany, NY, USA, in 1976, and the Ph.D. degree in physics from Princeton University, Princeton, NJ, USA, in 1980.

He has been with the Jet Propulsion Laboratory, Pasadena, CA, USA, since 1981. Over the last 35 years, he has contributed to the development of science algorithms for the NSCAT and SeaWinds ocean vector wind scatterometer projects. Since 2009, he has also been working on SMAP soil moisture and freeze-thaw algorithm development.

Andreas Colliander (Senior Member, IEEE) received the M.Sc. (Tech.), Lic.Sc. (Tech.), and D.Sc. (Tech.) degrees from the Helsinki University of Technology (TKK; now Aalto University), Espoo, Finland, in 2002, 2005, and 2007, respectively.

He is currently a Research Scientist with the Jet Propulsion Laboratory, California Institute of Technology, Pasadena, CA, USA. He is also leading the calibration and validation of the geophysical retrievals of the NASA's SMAP Mission. His research is focused on development of microwave remote sensing techniques.

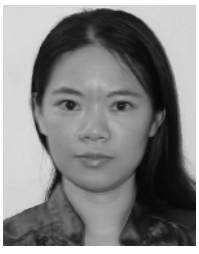

Fan Chen received the Ph.D. degree in climatology from the University of North Carolina, Chapel Hill, NC, USA, in 2006.

She is currently a Visiting Scientist with the Hydrology and Remote Sensing Laboratory, Agriculture Research Services (ARS), U.S. Department of Agriculture, Beltsville, MD, USA. Her research involves validation methodology for satellite retrievals of geophysical variables and application of data assimilation techniques to leverage satellite surface soil moisture products in hydrologic predictions.

Steven K. Chan (Senior Member, IEEE) received the Ph.D. degree in electrical engineering, specializing in electromagnetic wave propagation in random media, from the University of Washington, Seattle, WA, USA, in 1998.

He is currently a Research Scientist with the NASA Jet Propulsion Laboratory, California Institute of Technology, Pasadena, CA, USA. His work in soil moisture retrieval algorithm development encompasses the NASA Aqua/AMSR-E from 2002 to 2011, the JAXA GCOM-W/AMSR2 since 2012, and the NASA Soil Moisture Active Passive (SMAP) Mission since 2015. His research interests include microwave remote sensing of soil moisture and vegetation properties and their applications.

Dara Entekhabi (Fellow, IEEE) received the B.S. and M.S. degrees in geography from Clark University, Worcester, MA, USA, in 1983, 1985, and 1988, respectively, and the Ph.D. degree in civil and environmental engineering from the Massachusetts Institute of Technology (MIT), Cambridge, MA, USA, in 1990.

He is currently a Professor with the Department of Civil and Environmental Engineering and with the Department of Earth, Atmospheric and Planetary Sciences, MIT. He is also the Science Team Lead of the National Aeronautics and Space Administration's Soil Moisture Active and Passive (SMAP) Mission that was launched in January 2015. His research interests include terrestrial remote sensing, data assimilation, and coupled land-atmosphere systems modeling.

Dr. Entekhabi is a fellow of the American Meteorological Society and the American Geophysical Union. He is also a member of the National Academy of Engineering.

Rajat Bindlish (Senior Member, IEEE) received the B.S. degree in civil engineering from IIT Bombay, Mumbai, India, in 1993, and the M.S. and Ph.D. degrees in civil engineering from Pennsylvania State University, State College, PA, USA, in 1996 and 2000, respectively.

He is currently with the NASA Goddard Space Flight Center, Greenbelt, MD, USA. Prior to this, he was with the USDA Agricultural Research Service, Hydrology and Remote Sensing Laboratory, Beltsville, MD. He is currently working on soil moisture estimation from microwave sensors and their subsequent application in land surface hydrology. His research interest involves the application of microwave remote sensing in hydrology.

Dr. Bindlish is a member of the American Geophysical Union. He is also a Science Team Member of SMAP, NISAR, and Aquarius and GCOM-W missions.

Peggy E. O'Neill (Fellow, IEEE) received the B.S. degree *(summa cum laude)* (Hons.) in geography from Northern Illinois University, DeKalb, IL, USA, in 1976, the M.A. degree in geography from the University of California at Santa Barbara, Santa Barbara, CA, USA, in 1979, and the master's degree in civil and environmental engineering from Cornell University, Ithaca, NY, USA, in 1980.

Since 1980, she has been employed as a Research Physical Scientist with the Hydrological Sciences Laboratory, NASA Goddard Space Flight Center, Greenbelt, MD, USA, where she conducts research in soil moisture retrieval and land surface hydrology, primarily through microwave remote sensing techniques.

Dr. O'Neill was a recipient of the NASA Outstanding Performance and Special Achievement Awards, the Robert H. Goddard Award of Merit, the 2016 Federal Laboratory Consortium (FLC) Interagency Partnership Group Award, the USDA Certificate of Appreciation, and the 1994 IGARSS Symposium Prize Paper Award (as a coauthor). She is currently the SMAP Deputy Project Scientist.

Jun Asanuma received the B.Eng. and M.Eng. degrees in civil engineering from the University of Tokyo, Tokyo, Japan, in 1989 and 1991, respectively, and the Ph.D. degree in civil and environmental engineering from Cornell University, Ithaca, NY, USA, in 1996.

After having worked at the Central Research Center of Nippon Koei Company Ltd., Tokyo, as a Research Engineer in hydrology, he joined the Department of Civil and Environmental Engineering, Nagaoka University of Technology, Nagaoka, Japan. He moved to the Terrestrial Environmental Research Center, University of Tsukuba, Tsukuba, Japan, as a Lecturer, in 2000. His research interests include land surface hydrology, with emphases on the exchange of mass and energy between the land and the atmosphere through turbulence theories, modeling techniques, and field measurement techniques.

Aaron A. Berg received the B.Sc. and M.Sc. degrees in geography from the University of Lethbridge, Lethbridge, AB, Canada, in 1995 and 1997, respectively, the M.S. degree in geological sciences from The University of Texas at Austin, Austin, TX, USA, in 2001, and the Ph.D. degree in Earth system science from the University of California at Irvine, Irvine, CA, USA, in 2003.

Since 2003, he has been with the Department of Geography, Environment and Geomatics, University of Guelph, Guelph, ON, Canada. He teaches physical geography, hydrology, and remote sensing with research interests focused on the modeling and observation of soil moisture.

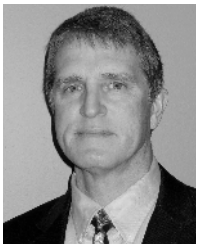

David D. Bosch received the Ph.D. degree in hydrology from The University of Arizona, Tucson, AZ, USA, in 1990.

In 1986, he joined the Agricultural Research Service. He leads a Watershed Research Program investigating the impacts of land use on water balance and quality. He has been active in the validation of remotely sensed soil moisture products since 2000. He is currently a Research Hydrologist with the Southeast Watershed Research Laboratory, Agricultural Research Service, Tifton, Georgia, USA. His primary research interests include watershed and landscape scale hydrology, agricultural impacts on water quality, hydrologic and solute transport modeling of watershed processes, riparian buffer hydrology and solute transport, and developing new methods for assessing the impact of agricultural chemicals on ground and surface water supplies.

Todd Caldwell received the B.S. degree in geosciences from The University of New Mexico, Albuquerque, NM, USA, in 1997, and the M.S. and Ph.D. degrees in hydrogeology from the University of Nevada at Reno, Reno, NV, USA, in 1999 and 2011, respectively.

He is currently a Hydrologist with the U.S. Geological Survey in the Nevada Water Science Center, Carson City, NV, USA. He specializes in the field of investigations and numerical modeling associated with near-surface vadose zone processes. While at UT-Austin, he was the Principal Investigator for the Texas Soil Observation Network (TxSON), one of 13 Core Validation Sites for NASA's Soil Moisture Active Passive Satellite Mission. His research focuses on *in situ* soil moisture monitoring, near surface geophysics, and spatial scaling.

Michael H. Cosh (Senior Member, IEEE) received the Ph.D. degree in civil and environmental engineering from Cornell University, Ithaca, NY, USA, in 2002.

He is currently a Research Hydrologist with the U.S. Department of Agriculture, Agricultural Research Service, Hydrology and Remote Sensing Laboratory, Beltsville, MD, USA. His current research interest includes the monitoring of soil moisture from both *in situ* resources and satellite products.

Chandra Holifield Collins received the Ph.D. degree in soil, water, and environmental science from the University of Arizona, Tucson, AZ, USA, in 2006. She is currently a Soil Scientist with the USDA-Agricultural Research Service, Southwest Watershed Research Center, Tucson. Her research interests include image analysis and the use of remote sensing data for agricultural applications, with current focus on operational tools for rangeland management.

José Martínez-Fernández received the B.S. degree in physical geography, the M.S. degree in water science and technology, and the Ph.D. degree in physical geography from the Universidad de Murcia (UM), Murcia, Spain, in 1985, 1991, and 1992, respectively.

He was a Research Fellow from 1988 to 1992 and a Junior Researcher from 1992 to 1994 with the Department of Geography, UM. He was an Assistant Professor in 1995 and an Associate Professor in 1997 with the Department of Geography, Universidad de Salamanca (USAL), Salamanca, Spain, where he has been a Professor of physical geography since May 2018. He is currently the Principal Investigator (PI) of the Water Resources Research Group, Instituto Hispano Luso de Investigaciones Agrarias (CIALE), USAL.

Dr. Martínez-Fernández has been a member of the Spanish National Biodiversity, Earth Sciences and Global Change Programme Research and Development Projects Selection Committee.

Mark Seyfried, photograph and biography not available at the time of publication.

Patrick J. Starks received the B.S. degree in physical geography from the University of Central Arkansas, Conway, AR, USA, in 1979, the M.A. degree in physical geography from the University of Nebraska-Omaha, Omaha, NE, USA, in 1984, and the Ph.D. degree in agronomy from the University of Nebraska-Lincoln, Lincoln, NE, in 1990.

From 1990 to 1992, he was a Post-Doctoral Fellow with the Department of Atmospheric Science, University of Missouri, Columbia, MO, USA. Since 1992, he has been with the USDA Agricultural Research Service, Beltsville, MD, USA, as a Research Soil Scientist and is stationed at the Grazinglands Research Laboratory, El Reno, OK, USA. His research activities span the areas of hydrology, soil science, and remote sensing.

Zhongbo (Bob) Su received the M.Sc. degree in hydrological engineering from IHE Delft, Delft, The Netherlands, in 1989, and the Ph.D. degree in civil engineering from Ruhr-Universität Bochum, Bochum, Germany, in 1996.

He is currently a Professor of spatial hydrology and water resources management and the Chairman of the Department of Water Resources, Faculty of Geo-Information Science and Earth Observation, University of Twente, Enschede, The Netherlands. His research focuses on remote sensing and numerical modeling of land surface processes and interactions with the atmosphere, Earth observation of water cycle and applications in climate, ecosystem and water resources studies, and monitoring food security and water-related disasters.

Marc Thibeault received the B.Sc. degree in physics from Laval University, Quebec City, QC, Canada, in 1982, the B.Sc. degree in mathematics from the University of Montreal, Montreal, QC in 1988, and the Dc. Science degree from the University of Buenos Aires, Buenos Aires, Argentina, in 2004.

He currently holds the position of the Head of the SAOCOM Project Science Group, a new L-Band mission of the Argentinian Space Agency. His research interests are on soil moisture, polarimetry, and other SAR applications.

Jeffrey Walker received the B.E. degree (Hons.) in civil engineering and the B.Surveying degree from the University of Newcastle, Callaghan, NSW, Australia, in 1995, and the Ph.D. degree in water resources engineering from the University of Newcastle in 1999. His Ph.D. thesis was among the early pioneering research on estimation of root-zone soil moisture from assimilation of remotely sensed surface soil moisture observations.

He then joined the NASA Goddard Space Flight Centre, Greenbelt, MD, USA, to implement his soil moisture work globally. In 2001, he moved to the Department of Civil and Environmental Engineering, University of Melbourne, Melbourne, VIC, Australia, as a Lecturer, where he continued his soil moisture work, including development of the only Australian airborne capability for simulating new satellite missions for soil moisture. In 2010, he was appointed as a Professor with the Department of Civil Engineering, Monash University, Melbourne, where he is continuing this research. He is contributing to soil moisture satellite missions at NASA, ESA, and JAXA, as a Science Team Member for the Soil Moisture Active Passive (SMAP) mission and a Cal/val Team Member for the Soil Moisture and Ocean Salinity (SMOS) and Global Change Observation Mission-Water (GCOM-W), respectively.

Dr. Walker received the Medal for the B.Surveying degree from the University of Newcastle.